JACS
JOURNAL OF THE AMERICAN CHEMICAL SOCIETY

Communication

pubs.acs.org/JACS

FePt Nanoparticles Assembled on Graphene as Enhanced Catalyst for Oxygen Reduction Reaction

Shaojun Guo and Shouheng Sun*

Department of Chemistry, Brown University, Providence, Rhode Island 02912, United States

Supporting Information

ABSTRACT: Seven-nanometer FePt nanoparticles (NPs) were synthesized and assembled on graphene (G) by a solution-phase self-assembly method. These G/FePt NPs were a more active and durable catalyst for oxygen reduction reaction (ORR) in 0.1 M $HClO_4$ than the same NPs or commercial Pt NPs deposited on conventional carbon support. The G/FePt NPs annealed at 100 °C for 1 h under Ar + 5% H_2 exhibited specific ORR activities of 1.6 mA/cm^2 at 0.512 V and 0.616 mA/cm^2 at 0.557 V (vs Ag/AgCl). As a comparison, the commercial Pt NPs (2−3 nm) had specific activities of 0.271 and 0.07 mA/cm^2 at the same potentials. The G/FePt NPs were also much more stable in the ORR condition and showed nearly no activity change after 10 000 potential sweeps. The work demonstrates that G is indeed a promising support to improve NP activity and durability for practical catalytic applications.

Graphene (G) is a two-dimensional single-layer sheet of graphite with p-electrons fully delocalized on the graphitic plane. It is highly conductive and mechanically strong and has been explored extensively for molecular electronic device, energy transfer, energy storage, and catalytic applications.[1] In catalytic studies, G is often used as a support, and its close contact with catalysts is believed to play an important role in activity enhancement of the catalyst. This has been demonstrated in the Pt (or Pd)-based nanoparticle (NP) catalysts grown on G for electrocatalytic reactions[2,3] and in the activation of Co_3O_4 and MoS_2 NPs by G for oxygen reduction reaction (ORR) in alkaline media[4] and for hydrogen evolution in H_2SO_4 solution.[5] In these studies, the catalyst NPs were grown directly on the G surface to maximize G−NP contact and to achieve the desired catalysis enhancement. However, the NPs prepared from the *in situ* growth method lack the desired size and morphology controls, and as a result, their catalytic potentials may not be fully realized. Considering the recent progress in solution-phase synthesis of monodisperse NPs, one would expect assembly of these NPs on the G surface to be a better approach to G/NPs for NP catalysis optimization. Despite various efforts in depositing NPs on solid supports, there has no report on controlled assembly of monodisperse NPs on G for catalytic applications.

Here we demonstrate that monodisperse FePt NPs can be self-assembled on G and show much enhanced activity and durability for ORR in $HClO_4$ solution. Recent studies have shown that MPt NP catalysts, especially those with M = Fe, Co, Ni, are active catalysts for ORR.[6,7] However, these MPt catalysts deposited on conventional carbon supports are not stable in acidic ORR conditions, and M tends to be etched away, leading to NP deterioration and catalytic activity reduction. In studying carbon support effects on FePt NP catalysis for ORR, we found a solution-phase-based self-assembly approach to deposit FePt NPs on G. These G/FePt NPs displayed higher ORR activity than either carbon (Ketjen EC-300J)-supported FePt NPs (C/FePt) or commercial C/Pt NPs in 0.1 M $HClO_4$, and this activity was further enhanced by annealing the G/FePt under Ar + 5% H_2 at 100 °C for 1 h. The G/FePt NPs were also stable under ORR conditions and showed nearly no activity change after 10 000 potential sweeps. The work demonstrates that G is indeed a promising support to improve NP catalytic activity and durability for practical catalytic applications.

The FePt NPs were synthesized as reported[8] with a slight modification, in which 220 °C, instead of 240 °C, was used for the NP growth. The FePt NP composition was analyzed by inductively coupled plasma−atomic emission spectroscopy (ICP-AES). With the amount of platinum(II) acetylacetonate, $Pt(acac)_2$, fixed at 0.2 g, adding 0.2 mL of $Fe(CO)_5$ led to 7 nm polyhedral $Fe_{58}Pt_{42}$ NPs, while 0.14 mL of $Fe(CO)_5$ resulted in $Fe_{42}Pt_{58}$ nanocubes (NCs) with edges of ∼7 nm. G was prepared by dimethylformamide (DMF) reduction of graphene oxide (GO) at ∼150 °C (see the Supporting Information)[9] and dispersed in DMF (Figure S1). The corresponding X-ray photoelectronic spectroscopy (Figure S2) and electrochemical impedance spectroscopy (Figure S3) of G and GO prove that G is successfully prepared. The FePt NPs were assembled on G surface as follows: 15 mg of the FePt NPs dispersed in 20 mL of hexane was added into 20 mL of DMF solution of G (0.5 mg/mL), and the mixture was sonicated for 1 h. Ten milliliters of ethanol was added, and the suspension was centrifuged at 9500 rpm for 10 min to separate the G/FePt product from the non-colored solvents. Fifteen milligrams of FePt NPs was also deposited on 10 mg of Ketjen carbon via sonication to make C/FePt catalyst as reported previously.[10] ICP-AES analyses show that FePt takes 49.6% of the total weight in G/FePt and 50.3% in C/FePt catalysts.

The FePt NPs and G/FePt NPs were characterized by transmission electron microscopy (TEM). Figure 1A is the typical TEM image of the 7 nm polyhedral $Fe_{58}Pt_{42}$ NPs deposited on an amorphous carbon-coated Cu grid. The NPs have a narrow size distribution with an average diameter of 7 ±

Received: November 7, 2011
Published: January 26, 2012

 © 2012 American Chemical Society dx.doi.org/10.1021/ja2104334 | J. Am. Chem.Soc. 2012, 134, 2492−2495

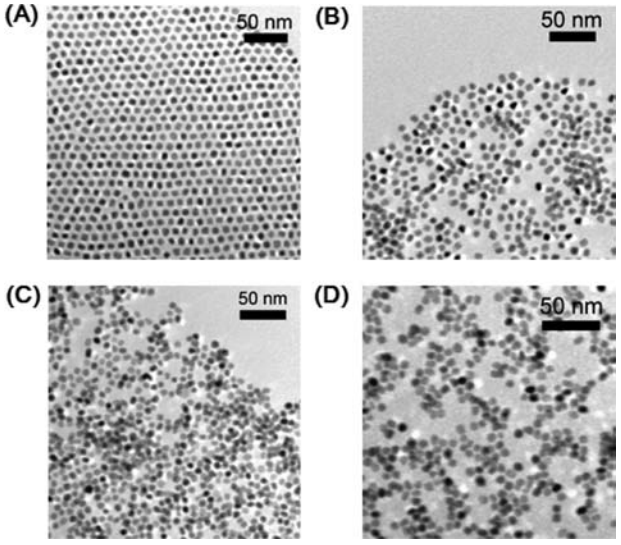

Figure 1. TEM images of (A) the 7 nm $Fe_{58}Pt_{42}$ NPs assembled on the amorphous carbon surface, (B) the $Fe_{58}Pt_{42}$ NPs assembled on the G surface, giving G/$Fe_{58}Pt_{42}$ NPs, (C) the G/$Fe_{58}Pt_{42}$ NPs after acetic acid wash, resulting in G/$Fe_{22}Pt_{78}$ NPs, and (D) the G/$Fe_{22}Pt_{78}$ NPs annealed under Ar + 5% H_2 at 100 °C for 1 h.

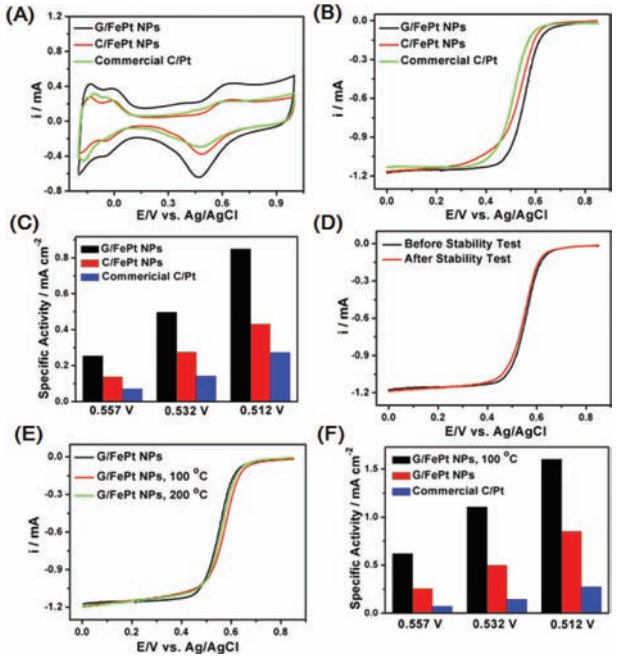

Figure 2. (A) CVs in N_2-saturated 0.1 M $HClO_4$ solution at a scan rate of 50 mV/s. (B) Polarization curves for ORR in O_2-saturated 0.1 M $HClO_4$ solution at 295 K. The potential scan rate was 10 mV/s and the electrode rotation speed was 1600 rpm. (C) ORR specific activities of the G/$Fe_{22}Pt_{78}$, C/$Fe_{24}Pt_{76}$, and commercial C/Pt catalysts, with Pt loading amounts of 14.3, 14.6, and 8 μg, respectively. (D,E) ORR polarization curves of (D) the G/$Fe_{22}Pt_{78}$ NPs before and after 10 000 potential sweeps between 0.4 and 0.8 V and (E) the G/$Fe_{22}Pt_{78}$ NPs annealed at different temperatures. (F) Comparison of ORR specific activities of the G/$Fe_{22}Pt_{78}$ NPs, the G/$Fe_{22}Pt_{78}$ NPs annealed 100 °C, and the commercial C/Pt catalyst.

0.5 nm. The X-ray diffraction (XRD) pattern of the NP assembly (Figure S4) shows that these FePt NPs have the face-centered cubic (fcc) structure. The as-prepared G sheets (Figure S5A) and G/FePt NPs are shown in Figures 1B and S5B,C. We can see that mixing the hexane dispersion of FePt NPs and the DMF solution of G sheets under sonication led to direct assembly of one layer of FePt NPs on G. In the NP assembly test, we could not obtain the monolayer assembly of FePt NPs by simply depositing the hexane dispersion of the FePt NPs on the G sheets—this direct deposition often led to uncontrolled FePt NP assembly on G. It appeared that mixing two immiscible solutions of FePt NPs (in hexane) and G (in DMF) via sonication was an essential step to assemble FePt NPs on G.

The G/FePt NPs were washed with 99% acetic acid (AA) at 70 °C to remove the surfactant around each FePt[10] and to ensure NP contact with G. ICP-AES analyses show that the washing led to partial loss of Fe in G/FePt and converted G/$Fe_{58}Pt_{42}$ NPs to G/$Fe_{22}Pt_{78}$ NPs. Despite this partial Fe loss, FePt NPs in G/FePt show no morphology change (Figure 1C). To make FePt NPs in even closer contact with G, we further annealed the G/FePt NPs under a gas mixture of Ar + 5% H_2 for 1 h. Compared to the un-annealed G/FePt NPs, the G/FePt NPs annealed at 100 °C show no morphology change (Figure 1D), but those annealed at 200 °C exhibit partial NP aggregation (Figure S6).

The G/FePt, C/FePt, and commercial C/Pt were redispersed in deionized water + isopropanol + 5% Nafion (v/v/v = 4/1/0.05) to reach a concentration of 2 mg/mL. Twenty-microliter portions of these dispersions were deposited on the surface of a glassy carbon (GC) electrode and dried under ambient conditions. Figure 2A shows the cyclic votammograms (CVs) of the AA-treated G/FePt (G/$Fe_{22}Pt_{78}$) NPs, C/FePt (C/$Fe_{24}Pt_{76}$) NPs, and commercial C/Pt catalyst in N_2-saturated 0.1 M $HClO_4$. The common hydrogen underpotential formation/stripping appears in the potential range of −0.2 to −0.15 V, the double-layer capacitance region locates from 0.2 to 0.4 V, and metal oxidation/reduction peaks are in the range 0.4−0.9 V. We can see that the double-layer capacitance of the G/FePt NPs is much larger than for C/FePt and the commercial C/Pt catalysts, indicating that G support has much larger surface area than the C support,[11] which is important for mass activity enhancement of Pt-based catalysts.

ORR measurements were performed in O_2-saturated 0.1 M $HClO_4$ solution using a GC rotating disk electrode at room temperature. Figure 2B shows the ORR polarization curves for the G/$Fe_{22}Pt_{78}$, C/$Fe_{24}Pt_{76}$, and commercial C/Pt catalysts. The polarization curves display the diffusion-limiting current region from −0.05 to 0.4 V and the mixed kinetic−diffusion control region between ∼0.5 and ∼0.7 V. The half-wave potential of G/FePt (0.557 V) is higher than those of C/FePt (0.532 V) and commercial C/Pt catalyst (0.512 V), indicating that G/FePt NPs have better electrocatalytic activity toward ORR than C/FePt NPs at the same Pt loading. The kinetic current was calculated from the polarization curve by considering the mass-transport correction and normalized with respect to electrochemical active surface area in order to compare the specific activity for different catalysts according to the Levich−Koutecky equation: $1/i = 1/i_k + 1/i_d$ (where i_k is the kinetic current and i_d is the diffusion-limiting current).[12] The ORR specific activity of different catalysts (Figure 2C) increases in the order G/FePt > C/FePt > C/Pt in the potential range of 0.512−0.557 V (vs Ag/AgCl). The mass activities of the above different catalysts also showed similar trends (see Figure S7). These comparisons indicate that G can effectively increase the activity of the FePt NPs. Durability tests

dx.doi.org/10.1021/ja2104334 | J. Am. Chem.Soc. 2012, 134, 2492−2495

were performed by cycling the potential between 0.4 and 0.8 V (vs Ag/AgCl) in O_2-saturated 0.1 M $HClO_4$ at a scan rate of 100 mV/s. Figure 2D shows the ORR activities for the G/FePt NPs before and after 10 000 potential sweeps. There is little change in ORR polarization curve and Fe/Pt composition (from 20/80 to 18/82) after these potential sweeps. Furthermore, there is no visible morphology change for FePt NPs after stability test (Figure S8). These suggest that G/FePt NPs are a class of stable catalysts for ORR. As a comparison, the commercial C/Pt NPs are not stable under the same reaction conditions, and their ORR polarization curve shows an obvious negative shift after stability test (Figure S9).

ORR activity of the annealed G/$Fe_{22}Pt_{78}$ NPs was also studied in 0.1 M $HClO_4$ solution (Figure 2E). We can see that the G/FePt NPs treated at 100 °C have even higher half-wave potential (0.575 V) than the AA-treated G/FePt NPs under the same detection conditions. However, the G/$Fe_{22}Pt_{78}$ NPs annealed at high temperature (200 °C) have a lower half-wave potential, due likely to the partial aggregation of the FePt NPs on the G sheet (Figure S6). The G/FePt NPs annealed at 100 °C have an ORR activity ~2 times high as for the AA-treated G/FePt NPs, 3.7−4.5 times high as for the C/FePt NPs, and 5.9−8.8 times as high as for the commercial C/Pt in the potential range of 0.512−0.557 V (Figure 2C,F).

The results from both activity and stability studies indicate that G has an important effect on ORR catalysis enhancement of FePt NPs. It seems that the close contact between G and FePt facilitates G's p-electron polarization from G to FePt (via a possible coordination bonding), making the FePt surface more easily accessible for O_2 absorption and activation. This polarization effect can be evidenced by the negative shift of the Pt reduction peak shown in Figure 2A and is facilitated by the controlled assembly of these FePt NPs on G and additional thermal annealing.

The G/FePt NPs also show the shape effect on ORR. It is known that Pt catalysts surrounded by (111) planes tend to be more active in $HClO_4$, while the cubic Pt catalysts are more active in H_2SO_4.[13] In current studies, we synthesized $Fe_{42}Pt_{58}$ NCs with an edge length of ~7 nm (Figure 3A) and assembled them on G followed by AA washing (Figure 3B), as described in the G/FePt NPs synthesis. The CVs and ORR polarization curves of the G/$Fe_{22}Pt_{78}$ NPs and G/$Fe_{18}Pt_{82}$ NCs in 0.1 M $HClO_4$ solution are shown in Figure S10. The half-wave potential of the G/FePt NPs is 0.557 V, which is more positive than that of the G/FePt NCs (0.545 V) (Figure S10B). Comparing ORR activities of the G/FePt catalysts (Figure 3C), we can see that the G/FePt NPs are more active than the G/FePt NCs in the 0.1 M $HClO_4$ solution. However, in the 0.5 M H_2SO_4 solution, the G/FePt NCs have better ORR activity than the G/FePt NPs (Figures 3D and S11). This agrees well with what has been observed on Pt NPs and Pt NCs,[13] indicating that G support does not change the shape-dependent FePt NP catalysis for ORR.

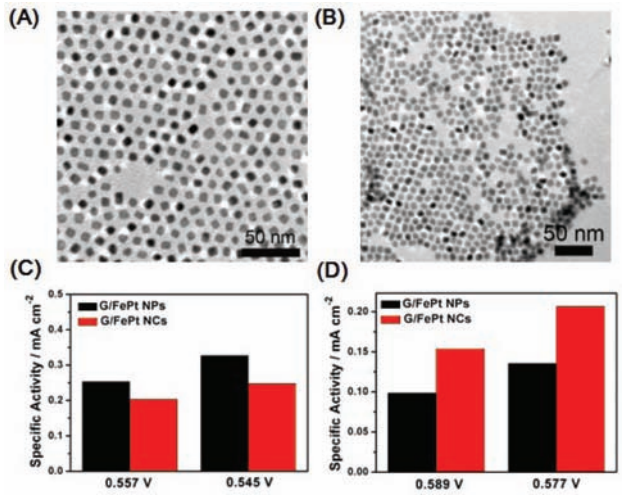

Figure 3. TEM images of (A) the $Fe_{42}Pt_{58}$ NCs and (B) the G/$Fe_{18}Pt_{82}$ NCs. ORR specific activity of the G/$Fe_{22}Pt_{78}$ NPs and the G/$Fe_{18}Pt_{82}$ NCs (C) in the O_2-saturated 0.1 M $HClO_4$ solution and (D) in the O_2-saturated 0.5 M H_2SO_4 solution.

In summary, we have developed a facile solution-phase self-assembly method to deposit FePt NPs on G surface. The G/FePt NPs show much enhanced catalytic activity and durability for ORR in 0.1 M $HClO_4$ solution. Especially, the G/FePt NPs annealed at 100 °C for 1 h have ORR activity about 2 times higher than the unannealed G/FePt NPs, 3.7−4.5 times higher than the C/FePt NPs, and 5.9−8.8 times higher than the commercial C/Pt NPs in the reduction potential range of 0.512−0.557 V (vs Ag/AgCl). The G/FePt NPs are stable under the ORR conditions and show nearly no activity change after 10 000 potential sweeps between 0.4 and 0.8 V. This work demonstrates that graphene is indeed a promising support to improve NP activity and durability for ORR. The reported self-assembly method can be generalized to produce various G/NPs for catalytic applications.

■ ASSOCIATED CONTENT

Ⓢ Supporting Information

FePt, graphene/FePt synthesis, and characterizations; Figures S1−11. This material is available free of charge via the Internet at http://pubs.acs.org.

■ AUTHOR INFORMATION

Corresponding Author

ssun@brown.edu

Notes

The authors declare no competing financial interest.

■ ACKNOWLEDGMENTS

Supported by the U.S. Department of Energy, Office of Energy Efficiency and Renewable Energy, Fuel Cell Technologies Program.

■ REFERENCES

(1) (a) Novoselov, K. S.; Geim, A. K.; Morozov, S. V.; Jiang, D.; Zhang, Y.; Dubonos, S. V.; Grigorieva, I. V.; Firsov, A. A. *Science* **2004**, *306*, 666−669. (b) Wang, H.; Cui, L.-F.; Yang, Y.; Casalongue, H. S.; Robinson, J. T.; Liang, Y.; Cui, Y.; Dai, H. *J. Am. Chem. Soc.* **2010**, *132*, 13978−13980. (c) Lv, W.; Tang, D.-M.; He, Y.-B.; You, C.-H.; Shi, Z.-Q.; Chen, X.-C.; Chen, C.-M.; Hou, P.-X.; Liu, C.; Yang, Q.-H. *ACS Nano* **2009**, *3*, 3730−3736. (d) Qu, L.; Liu, Y.; Baek, J.-B.; Dai, L. *ACS Nano* **2010**, *4*, 1321−1326. (e) Guo, S.; Dong, S. *Chem. Soc. Rev.* **2011**, *40*, 2644−2672.

(2) Guo, S.; Dong, S.; Wang, E. *ACS Nano* **2010**, *4*, 547−555.

(3) (a) Yoo, E.; Okata, T.; Akita, T.; Kohyama, M.; Nakamura, J.; Honma, I. *Nano Lett.* **2009**, *9*, 2255−2259. (b) Li, Y. M.; Tang, L. H.; Li, J. H. *Electrochem. Commun.* **2009**, *11*, 846−849. (c) Seger, B.; Kamat, P. V. *J. Phys. Chem. C* **2009**, *113*, 7990−7995. (d) Kou, R.; Shao, Y.; Mei, D.; Nie, Z.; Wang, D.; Wang, C.; Viswanathan, V.; Park, S.; Aksay, I. A.; Lin, Y.; Wang, Y.; Liu, J. *J. Am. Chem. Soc.* **2011**, *133*,

2541−2547. (e) Chen, X.; Wu, G.; Chen, J.; Chen, X.; Xie, Z.; Wang, X. *J. Am. Chem. Soc.* **2011**, *133*, 3693−3695.
(4) Liang, Y.; Li, Y.; Wang, H.; Zhou, J.; Wang, J.; Regier, T.; Dai, H. *Nat. Mater.* **2011**, *10*, 780−786.
(5) Li, Y.; Wang, H.; Xie, L.; Liang, Y.; Hong, G.; Dai, H. *J. Am. Chem. Soc.* **2011**, *133*, 7296−7299.
(6) (a) Wang, C.; Chi, M.; Wang, G.; van der Vliet, D.; Li, D.; More, K.; Wang, H.-H.; Schlueter, J. A.; Markovic, N. M.; Stamenkovic, V. R. *Adv. Funct. Mater.* **2010**, *21*, 147−152. (b) Yin, A.-X.; Min, X.-Q.; Zhang, Y.-W.; Yan, C.-H. *J. Am. Chem. Soc.* **2011**, *133*, 3816−3819. (c) Yang, H.; Zhang, J.; Sun, K.; Zou, S.; Fang, J. *Angew. Chem., Int. Ed.* **2010**, *49*, 6848−6851. (d) Zhang, J.; Yang, H.; Fang, J.; Zou, S. *Nano Lett.* **2010**, *10*, 638−644. (e) Wu, J.; Gross, A.; Yang, H. *Nano Lett.* **2011**, *11*, 798−802. (f) Kang, Y.; Murray, C. B. *J. Am. Chem. Soc.* **2010**, *132*, 7568−7569. (g) Xu, D.; Bliznakov, S.; Liu, Z.; Fang, J.; Dimitrov, N. *Angew. Chem., Int. Ed.* **2010**, *49*, 1282−1285. (h) Xu, D.; Liu, Z.; Yang, H.; Liu, Q.; Zhang, J.; Fang, J.; Zou, S.; Sun, K. *Angew. Chem., Int. Ed.* **2009**, *48*, 4217−4221.
(7) Stamenkovic, V. R.; Mun, B. S.; Arenz, M.; Mayrhofer, K. J. J.; Lucas, C. A.; Wang, G.; Ross, P. N.; Markovic, N. M. *Nat. Mater.* **2007**, *6*, 241−247.
(8) Kim, J.; Lee, Y.; Sun, S. *J. Am. Chem. Soc.* **2010**, *132*, 4996−4997.
(9) Ai, K. L.; Liu, Y. L.; Lu, L. H.; Cheng, X. L.; Huo, L. H. *J. Mater. Chem.* **2011**, *21*, 3365−3370.
(10) (a) Guo, S.; Zhang, S.; Sun, X.; Sun, S. *J. Am. Chem. Soc.* **2011**, *133*, 15354−15357. (b) Mazumder, V.; Sun, S. *J. Am. Chem. Soc.* **2009**, *131*, 4588−4589.
(11) Stoller, M. D.; Park, S.; Zhu, Y.; An, J.; Ruoff, R. S. *Nano Lett.* **2008**, *8*, 3498−3502.
(12) (a) Lim, B.; Jiang, M.; Camargo, P. H. C.; Cho, E. C.; Tao, J.; Lu, X.; Zhu, Y.; Xia, Y. *Science* **2009**, *324*, 1302−1305. (b) Zhang, H.; Jin, M.; Wang, J.; Li, W.; Camargo, P. H. C.; Kim, M. J.; Yang, D.; Xie, Z.; Xia, Y. *J. Am. Chem. Soc.* **2011**, *133*, 6078−6089.
(13) Wang, C.; Daimon, H.; Onodera, T.; Koda, T.; Sun, S. *Angew. Chem., Int. Ed.* **2008**, *47*, 3588−3591.